

Framework Cationization by Preemptive Coordination of Open Metal Sites for Anion-Exchange Encapsulation of Nucleotides and Coenzymes

Xiang Zhao, Chengyu Mao, Karen Tu Luong, Qipu Lin, Quan-Guo Zhai, Pingyun Feng, and Xianhui Bu*

Abstract: Cationic frameworks can selectively trap anions through ion exchange, and have applications in ion chromatography and drug delivery. However, cationic frameworks are much rarer than anionic or neutral ones. Herein, we propose a concept, preemptive coordination (PC), for targeting positively charged metal–organic frameworks (P-MOFs). PC refers to proactive blocking of metal coordination sites to preclude their occupation by neutralizing ligands such as OH^- . We use 20 MOFs to show that this PC concept is an effective approach for developing P-MOFs whose high stability, porosity, and anion-exchange capability allow immobilization of anionic nucleotides and coenzymes, in addition to charge- and size-selective capture or separation of organic dyes. The CO_2 and C_2H_2 uptake capacity of $117.9\text{ cm}^3\text{ g}^{-1}$ and $148.5\text{ cm}^3\text{ g}^{-1}$, respectively, at 273 K and 1 atm, is exceptionally high among cationic framework materials.

Crystalline porous materials (CPMs) with exchangeable ions are useful for many ion-exchange applications, such as pollutant extraction.^[1] In nature, CPMs (for example, zeolites) usually have an anionic framework. Cationic framework materials with anion exchange capability are desired for a variety of applications, such as removal of toxic ClO_4^- and AsO_4^{3-} , separation of nucleotides and amino acids, or immobilization of anionic pharmaceuticals.^[2]

Recent advances in MOFs have opened opportunities for developing P-MOFs.^[3] In fact, cationic frameworks were among the earliest MOFs to be studied.^[4] Examples include those formed by Cu^+ (or Ag^+) and neutral linkers, such as 4,4'-bipyridine. However, these P-MOFs have limited structural variety and low stability. One promising method for creating stable P-MOFs is to use clusters.^[5] But not all cluster types are

suitable, because of the extra attached negative ligands owing to the increased node connectivity, as well as the trapping of simple anions, such as O^{2-} , can make the overall charge of the cluster neutral or negative. It is the ratio between neutral and negative ligand groups that plays a pivotal role in the overall charge of a cluster. Synthetic strategies capable of controlling this ratio are thus desirable.

An analysis shows that both tetrameric $[\text{Zn}_4\text{O}(\text{RCOO})_6]$ and dimeric $\text{M}_2(\text{RCOO})_4(\text{solvent})_2$ clusters usually form neutral MOFs.^[6] In comparison, trigonal planar trimers could give a positive cluster, such as $[\text{M}_3\text{O}(\text{RCOO})_6\text{L}_3]^+$, when all of the M ions are trivalent and all of the L donor groups are neutral.^[7] There are, however, two pitfalls that could neutralize trimers: the inclusion of M^{2+} or the occupation of one L site by an anionic ligand (such as OH^-).^[8,9]

To overcome the neutralizing effect of M^{2+} , the simplest solution is to employ metal ions (such as In^{3+}) that are unlikely to exist as M^{2+} . However, it is advantageous to use transition metal ions because of their desirable properties, such as low cost, low toxicity, and high stability for applications in aqueous environments. Previous studies on trimers with ions such as Co and Ni often assign an ideal ratio of $\text{M}^{3+}/\text{M}^{2+}$ to make the cluster neutral.^[9–11] There are, however, no reasons why this must be the case. Here, we show that the $\text{M}^{3+}/\text{M}^{2+}$ ratio can deviate from the ideal value to give a cationic framework.

Additionally, even under the ideal all- M^{3+} conditions, $[\text{M}_3\text{O}(\text{RCOO})_6\text{L}_3]^+$ clusters can still be neutralized by coordinating anions. The concept of preemptive coordination (PC) involves the use of specially chosen ligands or ligand combinations with the goal to create 9-connected framework topologies in which all of the open metal sites of the trimer are occupied with neutral groups (Figure 1), precluding the attachment by neutralizing anions. This strategy is necessary because we cannot rely on solvent molecules, such as pyridine, to compete successfully against neutralizing anions, such as OH^- (Supporting Information, Scheme S1).

Herein, three topological types were used to show specific ways the PC concept can be implemented (Figure 1). One common feature in three topologies is the presence of two types of functional modules, a neutral pyridyl group (preemptive coordination module) and negative carboxylate groups (cluster-forming module), in a 1:2 ratio that was predetermined by the nature of the trimer. An intriguing aspect is the three different modes in which pyridyl and carboxylate groups are introduced.

[*] Dr. X. Zhao, K. T. Luong, Prof. Dr. X. Bu
Department of Chemistry and Biochemistry
California State University, Long Beach
1250 Bellflower Boulevard, Long Beach, CA 90840 (USA)
E-mail: xianhui.bu@csulb.edu

Dr. Q. Lin, Dr. Q.-G. Zhai, Prof. Dr. P. Feng
Department of Chemistry, University of California
Riverside, CA 92521 (USA)

C. Mao, Prof. Dr. P. Feng
Materials Science and Engineering Program
University of California
Riverside, CA 92521 (USA)

Supporting information and ORCID(s) from the author(s) for this article are available on the WWW under <http://dx.doi.org/10.1002/anie.201510812>.

Preemptive Coordination Strategy & Three Structural Examples

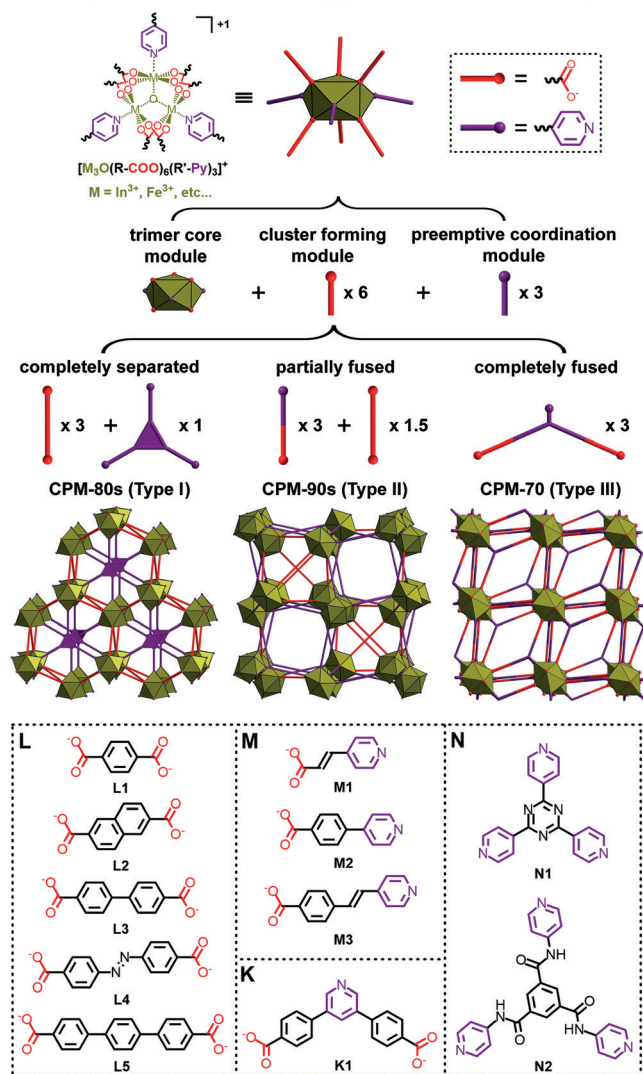


Figure 1. Coordination environment around trimers with preemptive coordination strategy (top) and 3 specific possibilities to construct cationic frameworks through preemptive coordination, according to the distribution of two functional modules in different ligand combinations (middle). The four types (L, M, K, N) of ligands used are shown (bottom).

The first mode involves the total separation of carboxylate and pyridine functionalities in two ligand types, resulting in structure type I (CPM-83 to CPM-89; Tables S1 and S2). This type consists of M^{3+} trimers, a linear dicarboxylate (L type), and a tritopic pyridine ligand (N type) in 1:3:1 ratio (Figures 1 and S8), leading to its general formula of $[(In_3O)(L)_3(N)](NO_3)$. This structure can be considered as the MIL-88 type with its open metal sites blocked by a tripyridine ligand. In the original MIL-88 type, the trimer is 6-connected and the open metal sites are occupied by neutral solvents or anions, such as Cl^- , rendering the framework either neutral or positive.^[9] With preemptive coordination, the pyridyl groups from the tripyridine ligand preoccupy all of the open metal sites, preventing such sites from being occupied by terminal anions (for example, OH^-), and leading to P-MOFs with the 9-connected trimer.

The second mode also involves the use of two types of ligands: isonicotinate-type (M type) and a linear dicarboxylate (L type). The resulting structure type II (CPM-91 to CPM-98; Tables S1 and S2) adopts the **ncb** net originally reported as a neutral framework owing to mixed-valence Ni trimer.^[10] This structure type has the general formula of $[In_3O(M)_3(L)_{1.5}](NO_3)$ (Figures 1 and S9). Similar to structure type I, the metal trimer is 9-connected. Therefore, the indium trimer and the entire framework are positively charged.

Unlike structure types I and II involving the co-assembly of two types of ligands, in structure type III (CPM-70, Tables S1 and S2), carboxylate and pyridyl functionality is fused in a single ligand (K type) in the 2:1 ratio (Figures 1 and S10), leading to a formula of $[In_3O(K)_3](NO_3)$. This structure type was known for Ni, Fe, Mg, and Co.^[11] While the Mg form is anionic, Fe, Co, and Ni forms were reported as neutral, owing to mixed M^{3+}/M^{2+} . Here, the all- M^{3+} system renders the framework positive.

A series of isorecticular structures have been synthesized from different ligand combinations (Tables S1 and S2). These frameworks contain apertures of different sizes and geometry, and can incorporate or exclude anionic guests according to their shape and size. These examples show great potential to prepare a library of P-MOFs with tunable pore properties, which are essential for applications as a selective ion exchanger or separation medium.

The P-MOFs reported here exhibit considerable porosity and large pore apertures, which allows for the incorporation of large organic species. For CPM-83-In, CPM-85-In, and CPM-87-In, the Langmuir surface areas determined from N_2 sorption isotherms are $1036.7 \text{ cm}^3 \text{ g}^{-1}$, $962.6 \text{ cm}^3 \text{ g}^{-1}$, and $1257.2 \text{ cm}^3 \text{ g}^{-1}$, respectively (Figure S4). They show high uptake capacity for CO_2 and C_2H_2 . At 273 K and 1 atm, the CO_2 uptake reaches $117.9 \text{ cm}^3 \text{ g}^{-1}$, $58.9 \text{ cm}^3 \text{ g}^{-1}$, and $34.4 \text{ cm}^3 \text{ g}^{-1}$, respectively. The corresponding values for C_2H_2 are $148.5 \text{ cm}^3 \text{ g}^{-1}$, $92.0 \text{ cm}^3 \text{ g}^{-1}$, and $76.0 \text{ cm}^3 \text{ g}^{-1}$.

Ion exchange of differently charged organic dyes was performed with CPM-85-In (Figure 2). A sample of CPM-85-In was immersed in a DMF solution of cationic methylene blue (MLB^+), neutral Sudan I (SDI^0), and anionic orange G (OG^{2-}), respectively, and UV/Vis absorbance was used to monitor their concentration changes over time. The results showed no obvious concentration change for MLB^+ and SDI^0 solution, indicating the absence of ion-exchange between NO_3^- and cationic or neutral dyes (Figure 2 b). In comparison, an obvious concentration drop was observed for OG^{2-} , and the color of the crystalline powder turned orange. This shows there was charge selectivity during ion exchange. It was further observed that, when the neutral nickel analogue was immersed in the OG^{2-} solution, no concentration change of OG^{2-} solution was observed (Figure 2 b), which again demonstrates ion exchange only occurs between hosts and guests of the opposite charge.

In addition to charge selectivity, CPM-85-In also exhibited size selectivity during ion exchange. Five anionic dyes with the same -2 charge, but different formula weight and size, were selected to probe the size selectivity. The dyes were orange G (OG^{2-}), ponceau 6R ($P6R^{2-}$), croscein scarlet 3B ($CS3B^{2-}$), croscein scarlet 7B ($CS7B^{2-}$), and acid blue 1 ($AB1^{2-}$;

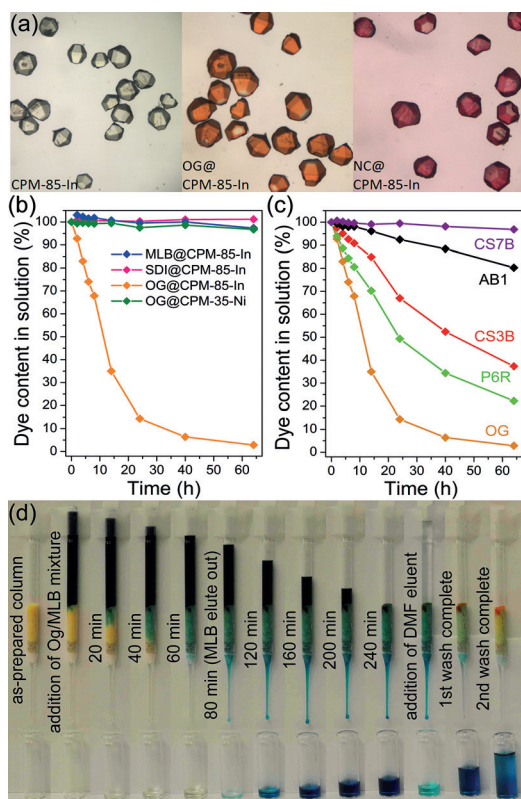


Figure 2. (a) Optical images of as-synthesized and dye-exchanged CPM-85. (b) The ion exchange is charge-dependent, shown by ion exchange of differently charged dyes in CPM-85 and its neutral nickel analogue. (c) The ion exchange process is size-dependent, demonstrated by different ion-exchange kinetics of five differently sized anionic dyes with the same charge. (d) Column chromatography showing the separation of the OG^{2-} /MLB $^{+}$ mixture. At the end of separation, the orange colored OG^{2-} was trapped at the top of column while the blue-colored MLB $^{+}$ eluted out. Chemical structures of dyes molecules are shown in Scheme S2.

Scheme S2). The concentration versus time plots of the five dyes show clear differences (Figure 2c), indicating size-dependent ion exchange kinetics.

Column chromatography, with an anion exchange column made of CPM-85-*In*, was used to show the separation process of a dye mixture (MLB $^{+}$ /OG $^{2-}$) based on their charge differences. As shown in Figure 2d, while the blue-colored MLB $^{+}$ eluted out immediately owing to the lack of ion exchange, the orange-colored negatively charged OG $^{2-}$ was trapped at the top of the column. Upon washing with excess amount of NaNO_3 solution, OG $^{2-}$ can be eluted out again. The efficient separation of MLB $^{+}$ and OG $^{2-}$ indicates P-MOFs can recognize and isolate charged organic species, which could lead to applications including selective trapping of drug molecules.

In this work, In^{3+} was studied first because its single crystal structure allows us to model other MOFs made in polycrystalline form, and because it is free from the neutralization effect of M^{2+} . For applications as an ion exchanger or separation medium, materials with lower cost, greater water stability, and biocompatibility are desirable. Here, a total of

11 polycrystalline Fe-MOFs in all three structure families were synthesized (Table S2). Their powder XRD patterns match well with those simulated from structural models based on In-MOFs (Figure S1–S3).

To test their stability, CPM-85-Fe and CPM-93-Fe were immersed in water for 3 weeks. The powder XRD before and after the treatments (Figure S5) shows little change in crystallinity. To test their stability under more harsh conditions, CPM-85-Fe was treated in aqueous acidic solution (pH 1) for 24 hours, or soaked in boiling water for 2 hours. Again, the sample remained intact after the treatment. Such high water and chemical stability renders them useful candidates for applications, such as enzyme immobilization, drug delivery, and ion chromatography.

Compared to In-MOFs, the framework charge of Fe-MOFs is not straightforward, owing to variable $\text{Fe}^{2+}/\text{Fe}^{3+}$ ratios. It is worth noting that to make P-MOFs, it is unnecessary to have 100% Fe^{3+} . For $[\text{M}_3\text{O}(\text{COO})_6]$, as long as the $\text{Fe}^{2+}/\text{Fe}^{3+}$ molar ratio falls into the range of 0–0.5, the framework would be positive, although the concentration of exchangeable anions would be affected by the $\text{Fe}^{2+}/\text{Fe}^{3+}$ ratio.

Previous studies were less concerned with the framework charge of the trimer-based structures because those reports did not focus on the ion exchange properties. For those containing metal ions with two possible oxidation states, an ideal ratio is often reported to give a neutral framework. In this work, we demonstrate a synthesis-based method for the evaluation of the framework charge.

Specifically, instead of directly determining the $\text{M}^{3+}/\text{M}^{2+}$ ratio, we focus on the concentration of charge-balancing anions. For this purpose, nitrate forms are not ideal, owing to difficulties in following the concentration changes of NO_3^- . Our method is based on the use of ClO_4^- salts, followed by elemental analysis using energy dispersive spectroscopy (EDS). By determining the Cl/Fe molar ratio, the charge of the framework can be estimated and the progress of ion exchange can be monitored. Table 1 summarizes the Cl/Fe molar ratio from the EDS study, which shows a significant amount of ClO_4^- counter anions, indicating these samples all have positively charged frameworks. For CPM-98-Fe, the Cl/Fe ratio is 0.33, indicating all of the Fe sites are in +3 state.

X-ray photoelectron spectroscopy (XPS) further confirmed the oxidation state of iron (Figure S11). The binding energy for Fe in CPM-92-Fe shows two characteristic peaks at 712.4 eV for Fe 2p $_{3/2}$ and 726.0 eV for Fe 2p $_{1/2}$, consistent with previously reported Fe^{3+} compounds. These values are larger than the characteristic peaks for Fe^{2+} compounds or mixed valence compounds, such as Fe_3O_4 . The presence of ClO_4^- was also confirmed with two peaks at 207.1 eV and 208.7 eV, consistent with the reported value for ClO_4^- .

The positive framework, together with the excellent water stability, offers these iron based P-MOFs great potential as cationic hosts for incorporation of various anionic species. Here, we demonstrate the ability of these Fe-MOFs to incorporate large anionic biomolecules, such as nucleotides and coenzymes including NADP and FAD, which play key roles in metabolism and enzymatic reactions in biosystems. The immobilization of these molecules into solid substrates can lead to enhanced resistance to environmental changes,

Table 1: Characterization of Fe-MOF samples by elemental analysis with EDS.

MOF	Atom % ^[a]		Cl/Fe ratio		Proposed Formula ^[b]
	Fe	Cl	Trial	Avg.	
CPM-95-Fe	1.77	0.31	0.175	0.177	[Fe ^{III} _{2.53} Fe ^{II} _{0.47} O(pba) ₃ (ndc) _{1.5}](ClO ₄) _{0.53}
	1.01	0.18	0.178		
CPM-97-Fe	1.21	0.35	0.289	0.274	[Fe ^{III} _{2.82} Fe ^{II} _{0.18} O(pvba) ₃ (ndc) _{1.5}](ClO ₄) _{0.82}
	1.08	0.28	0.259		
CPM-98-Fe	0.80	0.26	0.325	0.332	[Fe ^{III} ₃ O(pvba) ₃ (bpdc) _{1.5}](ClO ₄)
	1.37	0.46	0.336		
CPM-85-Fe	1.24	0.31	0.250	0.250	[Fe ^{III} _{2.75} Fe ^{II} _{0.25} O(bpdc) ₃ (tpt) _{1.5}](ClO ₄) _{0.75}
	1.85	0.46	0.249		
CPM-70-Fe	1.65	0.12	0.0727	0.0721	[Fe ^{III} _{2.22} Fe ^{II} _{0.78} O(pbpc) ₃](ClO ₄) _{0.22}
	6.15	0.44	0.0715		

[a] Two separate areas of each sample were selected for elemental analysis by EDS. [b] Full names of abbreviations used here can be found in Table S2.

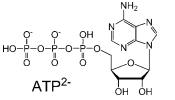
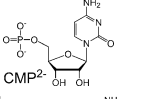
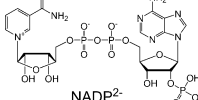
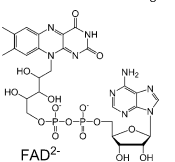
which is desirable for applications in drug delivery and catalytic reactions.

CPM-97-Fe and CPM-98-Fe were selected in this study owing to their large window apertures and channels. To monitor the anion exchange process, we focused on the nature of counter anions within the pores before and after anion exchange. In this case, the exchangeable anion in CPM-97-Fe and CPM-98-Fe is ClO₄[−], which is exchanged out by phosphate-containing anionic guests. EDS was used to monitor the change of Cl/Fe and P/Fe ratios during ion exchange. For all four of the host–guest combinations studied here, a dramatic decrease in the Cl/Fe ratio, coupled with simultaneous increase in the P/Fe ratio were observed, which reveals the anion exchange nature of the process (Table 2). The total charge of exchanged-out ClO₄[−] is approximately balanced by exchanged-in anions. To evaluate the extent of ion exchange, the fraction of the exchanged-out ClO₄[−] to the total amount of ClO₄[−] in the original compound is used. The EDS results showed that all of the ion exchange processes reached near completion in a short amount of time. For

example, 97 % of ClO₄[−] in CPM-98-Fe was replaced by ATP^{2−} within 2 hours. Impressively, some large-sized dinucleotide-type coenzyme anions, such as NADP^{2−} and FAD^{2−}, can replace > 80 % of the original ClO₄[−] in CPM-97-Fe in a similar time scale. This ion exchange-based route represents a novel method for enzyme immobilization.

In summary, we demonstrate the use and effectiveness of the PC concept as a strategy to synthesize 20 new P-MOFs. The high stability, especially of Fe-MOFs in aqueous media, makes them promising candidates for biocompatible applications. The charge- and size-selective anion exchange, separation, or immobilization of organic dyes, nucleotides, and coenzymes was demonstrated. A method for estimating the degree of framework cationization and related anion exchange capacity, as well as for monitoring the anion exchange process, was also demonstrated by tracking charge-balancing anions. We believe this materials design and synthesis strategy can lead to the development of a large number of useful P-MOF materials for various applications.

Table 2: Ion exchange-promoted immobilization of nucleotides and redox coenzymes.

P-MOF	Anionic Guest	Cl/Fe ratio		P/Fe ratio		Extent of Ion Exchange [%]	Loading Amount [mg g ^{−1}]
		initial	final	initial	final		
CPM-98-Fe		0.3318	0.0083	0	0.5058	97.5	203.2
CPM-97-Fe		0.2743	0.0228	0	0.1236	91.7	206.4
CPM-97-Fe		0.2743	0.0467	0	0.3478	83.0	215.1
CPM-97-Fe		0.2743	0.0351	0	0.2281	87.2	238.5

Acknowledgements

This work was supported by National Science Foundation, Division of Materials Research, under Award #1309347. The gas sorption instrument was funded by W. M. Keck Foundation. XB thanks the RSCA award from CSULB.

Keywords: anion separation · cationic frameworks · ion exchange · metal–organic frameworks

How to cite: *Angew. Chem. Int. Ed.* **2016**, 55, 2768–2772
Angew. Chem. **2016**, 128, 2818–2822

-
- [1] a) S. R. J. Oliver, *Chem. Soc. Rev.* **2009**, 38, 1868; b) B. Li, Y. Zhang, D. Ma, Z. Shi, S. Ma, *Nat. Commun.* **2014**, 5, 5537; c) Q. Zhang, J. Yu, J. Cai, L. Zhang, Y. Cui, Y. Yang, B. Chen, G. Qian, *Chem. Commun.* **2015**, 51, 14732; d) D. F. Sava, M. A. Rodriguez, K. W. Chapman, P. J. Chupas, J. A. Greathouse, P. S. Crozier, T. M. Nenoff, *J. Am. Chem. Soc.* **2011**, 133, 12398; e) M. Carboni, C. W. Abney, S. Liu, W. Lin, *Chem. Sci.* **2013**, 4, 2396; f) Y. Lin, W. Massa, S. Dehnen, *J. Am. Chem. Soc.* **2012**, 134, 4497.
- [2] a) J. S. Lee, H. Luo, G. A. Baker, S. Dai, *Chem. Mater.* **2009**, 21, 4756; b) H.-R. Fu, Z.-X. Xu, J. Zhang, *Chem. Mater.* **2015**, 27, 205.
- [3] a) E. R. Parnham, R. E. Morris, *Acc. Chem. Res.* **2007**, 40, 1005; b) H.-Y. Lin, C.-Y. Chin, H.-L. Huang, W.-Y. Huang, M.-J. Sie, L.-H. Huang, Y.-H. Lee, C.-H. Lin, K.-H. Lii, X. Bu, S.-L. Wang, *Science* **2013**, 339, 811; c) Q. Lin, J. Lu, Z. Yang, X. C. Zeng, J. Zhang, *J. Mater. Chem. A* **2014**, 2, 14876; d) M. Kim, J. F. Cahill, H. Fei, K. A. Prather, S. M. Cohen, *J. Am. Chem. Soc.* **2012**, 134, 18082; e) J. Gao, J. Miao, P.-Z. Li, W. Y. Teng, L. Yang, Y. Zhao, B. Liu, Q. Zhang, *Chem. Commun.* **2014**, 50, 3786; f) H. Fei, J. F. Cahill, K. A. Prather, S. M. Cohen, *Inorg. Chem.* **2013**, 52, 4011.
- [4] B. F. Abrahams, S. R. Batten, M. J. Grannas, H. Hamit, B. F. Hoskins, R. Robson, *Angew. Chem. Int. Ed.* **1999**, 38, 1475; *Angew. Chem.* **1999**, 111, 1538.
- [5] a) A. Schoedel, L. Wojtas, S. P. Kelley, R. D. Rogers, M. Eddaoudi, M. J. Zaworotko, *Angew. Chem. Int. Ed.* **2011**, 50, 11421; *Angew. Chem.* **2011**, 123, 11623; b) S.-T. Zheng, X. Zhao, S. Lau, A. Fuhr, P. Feng, X. Bu, *J. Am. Chem. Soc.* **2013**, 135, 10270.
- [6] H. Li, M. Eddaoudi, M. O’Keeffe, O. M. Yaghi, *Nature* **1999**, 402, 276.
- [7] A. Schoedel, M. J. Zaworotko, *Chem. Sci.* **2014**, 5, 1269.
- [8] C. Mao, R. A. Kudla, F. Zuo, X. Zhao, L. J. Mueller, X. Bu, *J. Am. Chem. Soc.* **2014**, 136, 7579.
- [9] a) C. Serre, F. Millange, S. Surble, G. Férey, *Angew. Chem. Int. Ed.* **2004**, 43, 6285; *Angew. Chem.* **2004**, 116, 6445; b) A. C. Sudik, N. W. Ockwig, A. P. Côté, O. M. Yaghi, *Inorg. Chem.* **2005**, 44, 2998; c) X. Zhao, X. Bu, Q.-G. Zhai, H. Tran, P. Feng, *J. Am. Chem. Soc.* **2015**, 137, 1396.
- [10] a) Y.-B. Zhang, W. X. Zhang, F. Y. Feng, J. P. Zhang, X. M. Chen, *Angew. Chem. Int. Ed.* **2009**, 48, 5287; *Angew. Chem.* **2009**, 121, 5391; b) G. Jiang, T. Wu, S.-T. Zheng, X. Zhao, Q. Lin, X. Bu, P. Feng, *Cryst. Growth Des.* **2011**, 11, 3713; c) Y.-B. Zhang, H.-L. Zhou, R.-B. Lin, C. Zhang, J.-B. Lin, J.-P. Zhang, X.-M. Chen, *Nat. Commun.* **2012**, 3, 642; d) X. Zhao, X. Bu, T. Wu, S.-T. Zheng, L. Wang, P. Feng, *Nat. Commun.* **2013**, 4, 2344.
- [11] a) J. Jia, X. Lin, C. Wilson, A. J. Blake, N. R. Champness, P. Hubberstey, G. Walker, E. J. Cussen, M. Schröder, *Chem. Commun.* **2007**, 840; b) X.-M. Zhang, Y.-Z. Zheng, C.-R. Li, W.-X. Zhang, X.-M. Chen, *Cryst. Growth Des.* **2007**, 7, 980; c) Q.-G. Zhai, Q. Lin, T. Wu, S.-T. Zheng, X. Bu, P. Feng, *Dalton Trans.* **2012**, 41, 2866.

Received: November 25, 2015

Revised: December 31, 2015